Automotive Experiences
Vol. 7 No. 2 (2024) pp. 270-283
p-ISSN: 2615-6202 e-ISSN: 2615-6636

Research Paper

Design and Crash Test on a Two-Passenger City Car Frame using the Finite Element Method

Randi Purnama Putra[1,2], **Dori Yuvenda**[1,2], **Wanda Afnison**[1,2], **Remon Lapisa**[1,2], **Milana**[1,3], **Anna Niska Fauza**[1,2], **Dani Harmanto**[4]

[1]Transportation and Vehicle Research Group, Universitas Negeri Padang, Padang 25131, Indonesia
[2]Department of Mechanical Engineering, Universitas Negeri Padang, Padang 25131, Indonesia
[3]Department of Automotive Engineering, Universitas Negeri Padang, Padang 25131, Indonesia
[3]Department of Aeronautical Engineering, De Monfort University, Leicester LE1 9BH, United Kingdom

randipurnama@ft.unp.ac.id

https://doi.org/10.31603/ae.11306

Published by Automotive Laboratory of Universitas Muhammadiyah Magelang

Article Info
Submitted:
28/04/2024
Revised:
08/08/2024
Accepted:
09/08/2024
Online first:
18/09/2024

Abstract

Currently, more people utilize motorized cars annually, particularly passenger and commercial vehicles. This affects the amount of traffic in urban areas and the demand for parking places. One of the initiatives taken by the auto industry to address this issue is the introduction of a two-passenger minicar. The chassis is an important part of a car which must have a strong construction to withstand the weight of the vehicle. The purpose of this research is to create a city car's chassis that can hold two passengers and then crash-test the finished product. In this research, a development method was used using SolidWorks software and the student version of ANSYS R2 2023 as software for creating chassis designs and crash test simulations. The study's findings indicate that the car frame's measurements are 2.46 meters in length, 1.33 meters in height, and 1.39 meters in width. The steel of the ASTM A36 type was utilized as the material in the computational study of the frame. The results show that increasing speed causes an increase in deformation, with the peak deformation at a speed of 100 km/h. The maximum deformation occurs at 0.007 seconds with a value of 203.51 mm at the top pillar of the car. The deformation increases from 97.196 mm at 0.0035 s to 161.22 mm at 0.0056 s. However, deformation occurs mainly in the front zone of the car frame and is not significant in the passenger zone.

Keywords: Crash test; Car frame; Two passenger; City car; Finite element method

1. Introduction

The automotive industry has undergone transformative advancements in vehicle safety technology over the past several decades [1]–[3]. The evolution of safety features, from the airbags technology [4], structural design [5], [6], stability [7], braking systems [8], [9], collision avoidance technologies [10]–[12], to advanced materials [13]–[16], reflects the industry's commitment to enhancing occupant protection. However, despite these remarkable strides, two-passenger cars, with their unique design characteristics, present distinct safety challenges. Their smaller dimensions, reduced weight, and simpler structural frameworks compared to medium and large passenger vehicles can influence their crash performance, as smaller frames may be less effective at absorbing crash energy [17], [18]. Therefore, the goal of these innovations is to improve passenger safety and mitigate injury risks in crash scenarios.

Recent advancements in car frame design have become central to efforts aimed at improving vehicle safety [19]–[21]. Designing a frame that combines both strength and resistance to deformation is critical for ensuring passenger safety during collisions [22], [23]. Lightweight design approaches, while beneficial for fuel efficiency, may compromise structural integrity, potentially affecting the vehicle's ability to withstand impact forces. Therefore, achieving an optimal balance between frame strength and weight is especially crucial for two-passenger vehicles, which must effectively manage crash energy despite their compact size.

Crash testing remains a fundamental method in the development of safer vehicles [24]–[27]. Rigorous crash tests, conducted under a variety of conditions, provide essential insights into a vehicle's safety performance and enable manufacturers to implement necessary design improvements. Comprehensive crash testing protocols must address a range of collision types, including frontal, side, and oblique impacts. Despite extensive research into crash testing for general passenger cars, there is a notable lack of specific studies focusing on two-passenger vehicles [28]–[30]. This gap underscores the need for targeted research to better understand the crash performance of two-passenger cars and to develop strategies for enhancing their safety.

Two-passenger cars play a significant role in addressing daily mobility needs while offering optimal space utilization and fuel efficiency. The design of these vehicles must consider not only aesthetic factors but also critical safety aspects [31], [32]. Crash tests are pivotal for evaluating the performance and structural reliability of these car frames [33], [34]. While research on crash testing of passenger cars is extensive, studies specifically targeting two-passenger vehicles are limited. The absence of detailed data on how these vehicles respond to various crash scenarios poses a challenge, highlighting the necessity for focused research in this area. Furthermore, as automotive technology continues to evolve, recent design changes may not yet be fully represented in existing crash test data. Comparative analyses between two-passenger cars and their larger counterparts have also been insufficiently explored in the literature.

This research seeks to address these gaps by designing and testing a two-passenger car frame to evaluate its safety performance in crash situations. By advancing the understanding of how two-passenger cars perform during crashes, this study aims to contribute valuable insights to the development of safer vehicle designs and more effective safety strategies. The findings will be beneficial for both automakers, in the development of new, safer products, and regulatory agencies, in formulating improved safety standards. As technology and safety regulations continue to progress, this research is expected to offer a foundation for future advancements in vehicle design and crash testing methodologies. Ultimately, this study aims to pave the way for the creation of safer, more efficient, and environmentally friendly vehicles, aligning with the ongoing evolution of automotive safety and performance standards.

2. Methods

The research method used in this research is a numerical method using the finite element method. The numerical computing simulation process uses the student version of ANSYS R2 2023 software. This research stage begins with needs analysis, design and improvement, testing, and results (**Figure 1**). In the needs analysis stage, identification and analysis of needs are carried out in designing the frame of a two-passenger city car. This process involves a thorough literature review of vehicle safety standards, traffic accident research, as well as user preferences regarding safety features. After the needs analysis is identified, the frame design and development stages are carried out. Using Solidworks software, the car frame structure was designed. In this design process, the development of the frame was also carried out so that the frame design was suitable for a capacity of two passengers. After an adequate design was obtained, the testing phase was carried out with ANSYS R2 2023 software. The two-passenger city car frame was tested using the finite element method in a collision simulation, where the structure's response to collision forces was monitored and evaluated.

In this study, the method used for the crash test is the Frontal Crash Test in accordance with the standards set by the National Highway Traffic Safety Administration (NHTSA). The Frontal Crash Test aims to evaluate the safety performance of vehicles in frontal collisions, which are a common and often severe type of accident. The test process involves the vehicle being launched towards a fixed barrier or wall. while the material used for the car frame is A36 steel. A36 steel is a type of carbon steel that is commonly used in various structural and engineering applications due to its good mechanical properties and ease of processing. The properties data of A36 steel can be seen in **Table 1**.

The type of mesh is used tetrahedral unstructured to model the frame structure of a two-passenger city car. Detailed meshing is applied to critical areas such as joints and sharp corners to ensure adequate resolution. Grid independence analysis is an important step in validating simulation results [35], [36]. This is done by varying the size of the mesh elements and ensuring that changes in the mesh size do not significantly affect the results. This process begins by creating several models with different element sizes, starting from Mesh A to Mesh E (**Table 2**). Based on the results of the independence grid analysis, the type of mesh chosen in this research is mesh D because it has the smallest error. In **Figure 2** show that the deformation vs time between mesh D and previous research [37].

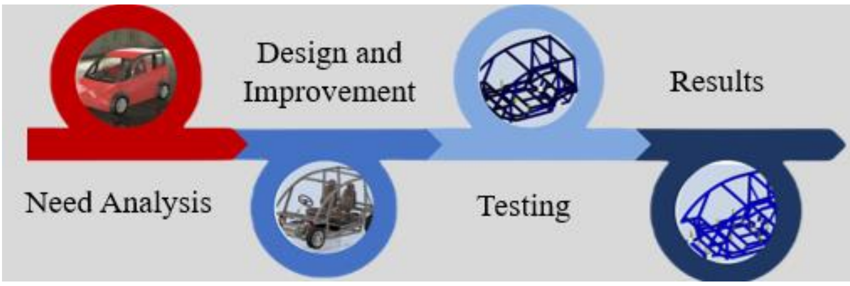

Figure 1. Research stages

Table 1. Properties of A36 steel material

Properties	A36 type-Steel
Density (g/cm^3)	7.80
Poisson ratio	0.26
Yield Strength (MPa)	250
Ultimate Tensile Strength (MPa)	550
Percentage Elongation	20

Table 2. Independence grid analysis

No	Type	Number of Elements	Internal Energy	Error (%)	Average deformation	Error (%)
1	Mesh A	4064	3797740	-	193.06	-
2	Mesh B	5068	3673088	3.28	196.66	1.86
3	Mesh C	6070	3604640	1.86	199.12	1.25
4	Mesh D	7032	3628618	0.67	200.84	0.86
5	Mesh E	8090	3050577	15.93	202.37	1.62

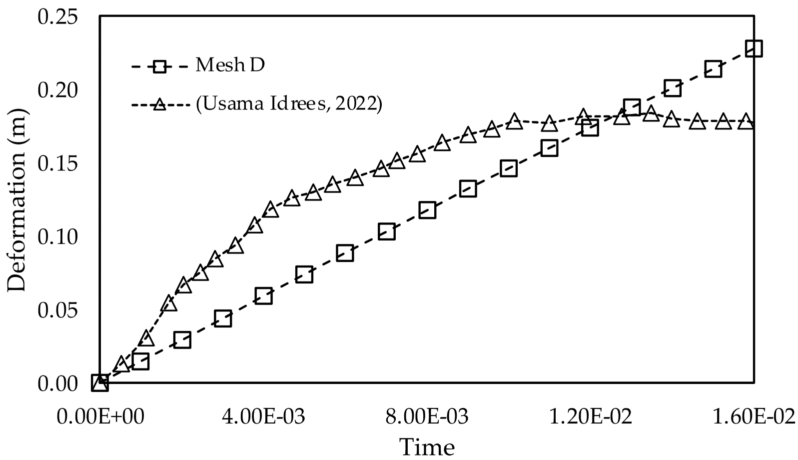

Figure 2. Deformation vs time between mesh D and previous research [37]

Furthermore, in this research, boundary conditions are a crucial factor in ensuring the accuracy of the simulation results. Boundary conditions in this research refer to the parameters or limits set for collision simulation or testing, which include various variables such as speed, barrier type, and collision mode. Setting the right boundary conditions is the basis for the simulation process in realistic crash testing and provides accurate data regarding the behavior of the car frame structure under certain conditions. The boundary conditions applied to the two-passenger car frame and boundary walls in this study are illustrated in **Figure 3** and explained in **Table 3**. As **Table 3** explains, the car structure is given varying speeds, and the boundary walls are blocked from all sides. In **Table 4** it can be seen that there are 4 crash test models used. Starting from speeds of 40 km/h, 64 km/h, 80 km/h and 100 km/h. The crash test model used is frontal impact.

3. Results and Discussion

This research aims to create a chassis design for an electric car with a capacity of 2 passengers and carry out tests in the form of crash tests on the chassis that has been created. In designing, research was carried out using SolidWorks software. For numerical simulation of crash tests on the chassis, use the student version of ANSYS R2 2023. The results achieved in this research include the frame design of a city car with a 3-dimensional model and crash test data on the chassis. The following describes the results that have been achieved.

3.1. *Chassis Design*

The dimensions of the car frame with a capacity of two passengers have a chassis length of 2.46 meters, height of 1.33 meters, and width of 1.39 meters. Length, height, and width are the main dimensions that determine the overall size and proportions of the car frame structure. The length of the chassis determines the distance between the front and back of the car, while the height and width of the chassis affect the overall height and width of the vehicle. The material used in the numerical analysis of this car frame is ASTM A36-type steel. ASTM A36 steel is one of the most commonly used types of structural steel in the construction and automotive industries because it has good strength and adequate toughness. The choice of ASTM A36 steel in the frame of this two-passenger car is used to ensure the strength and reliability of the structure, as well as allow a design that is light but remains sturdy and resistant to the loads imposed when the car is moving. The design of the chassis is shown in **Figure 4**.

Table 3. Details of boundary conditions

Name	Type	Condition
A	Fixed Support	Barrier Fix
B	Velocity	X direction Front

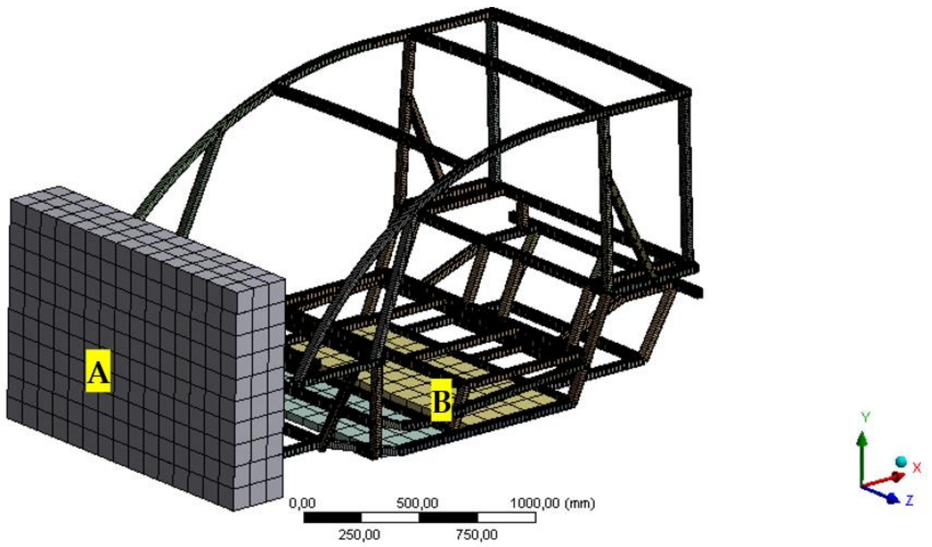

Figure 3. Bondary condition

Table 4. Crash test specifications for a car frame with a capacity of two passengers

Test Number	Weight of the entire vehicle	Mode	Speed
Test 1	507.6 kg	Frontal impact	40 km/h
Test 2	507.6 kg	Frontal impact	64 km/h
Test 3	507.6 kg	Frontal impact	80 km/h
Test 4	507.6 kg	Frontal impact	100 km/h

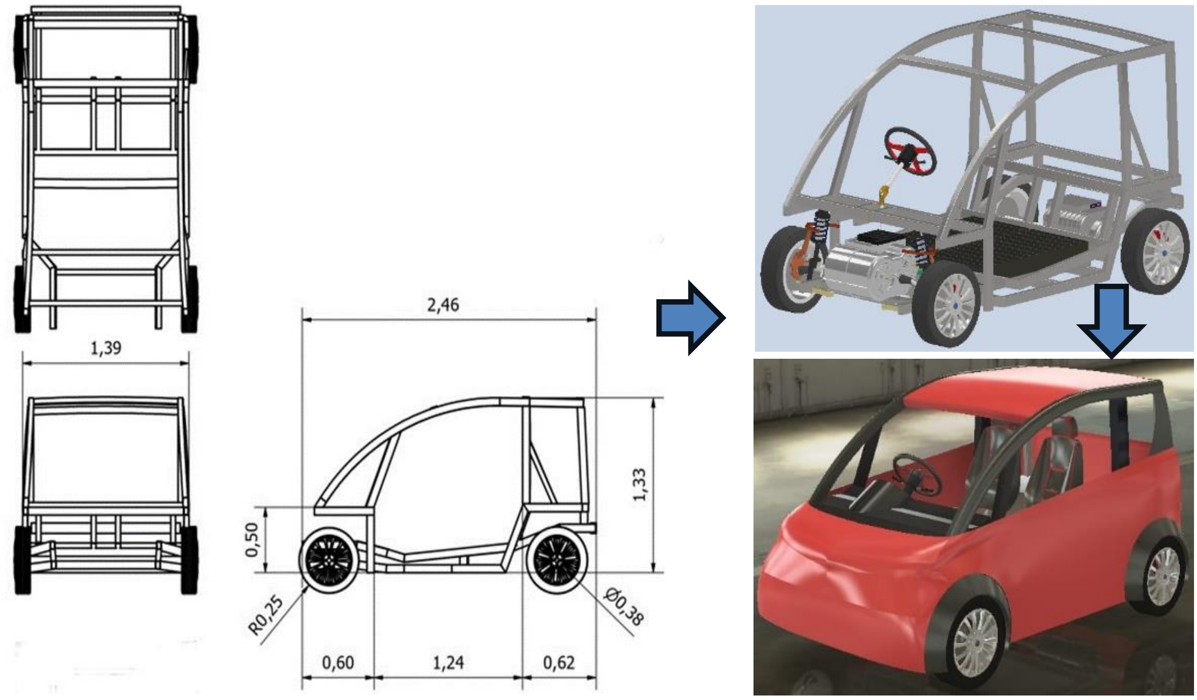

Figure 4. Chassis design for a two-passenger car in 2D and 3D (dimensions in m)

3.2. *Crash Test on Chassis*

3.2.1. *Crash Test at a Speed of 40 km/h*

This test was conducted in 1.7×10^{-2} seconds at a speed of 40 km/h. **Figure 5** displays the contours of the collision impact results on the car structure before and after investigation at different time steps. Since the car frame has not yet struck the barrier wall, no deformation occurs at the zero seconds displayed in **Figure 5a**. The contour in **Figure 5b** exhibits some distortion at time 0.008 s. At this point, the highest deformation measured was 88.88 mm. With an increase in time of 0.013 s, the maximum deformation that occurs reaches 148.85 mm **Figure 5c**. It can also be seen in **Figure 5c**. This means that as time increases, the deformation locations become evenly distributed in all parts of the chassis. In **Figure 5d**, the maximum deformation reaches its maximum value of 201.47 mm at the final time step of 0.017 s. **Table 5** tabulates these deformation values.

For further information, in **Figure 6** it can also be seen that the car chassis is experiencing local deformation. The maximum amount of deformation is 201.47 mm in the front zones of the chassis. The passenger roof frame zone has shifted slightly in shape and this deformation can be seen on the roof of the car frame. The energy balance graph is shown in **Figure 7** which shows the energy transformation. The car's kinetic energy decreases after hitting a wall. The automotive frame's elastic and plastic deformation causes a rise in internal energy.

3.2.2. *Crash Test at a Speed of 64 km/h*

In Test 2, the vehicle was driven at 64 km/h with a stopping time of 1.1×10^{-2} seconds. The collision impact effects on the car chassis before and after various studies and time steps are depicted by the contours in **Figure 8**.

Table 5. Deformation vs time at a speed of 40 km/h.

Time (s)	Maximum deformation (mm)
0	0
0.008	88.88
0.013	148.85
0.017	201.47

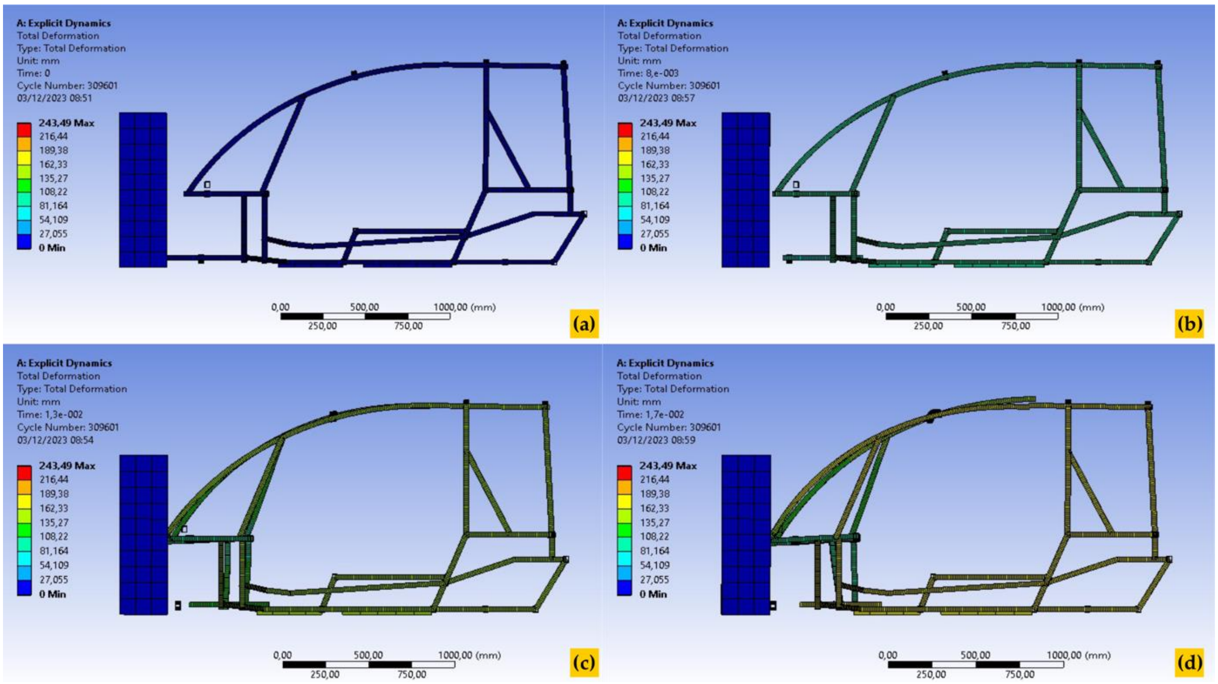

Figure 5. The car's chassis deformation: (a) 0 s; (b) 0.006 s; (c) 0.009 s; (d) 0.011 s.

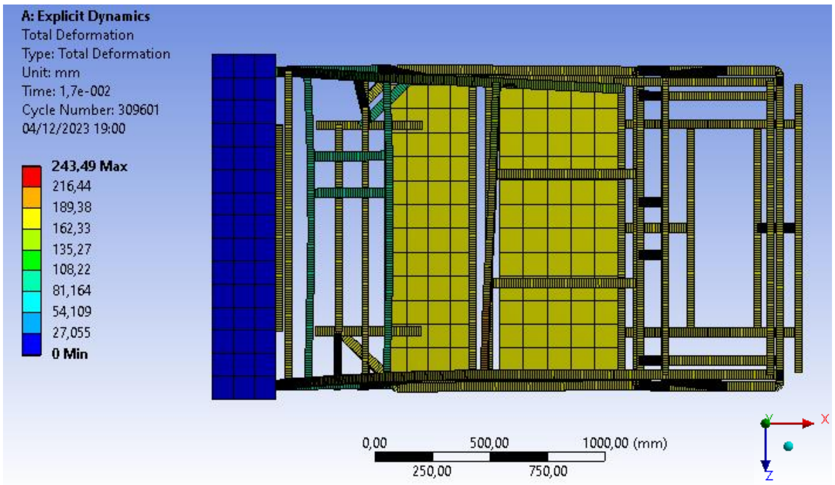

Figure 6. Deformation of the car chassis with time 0.017 s (top view)

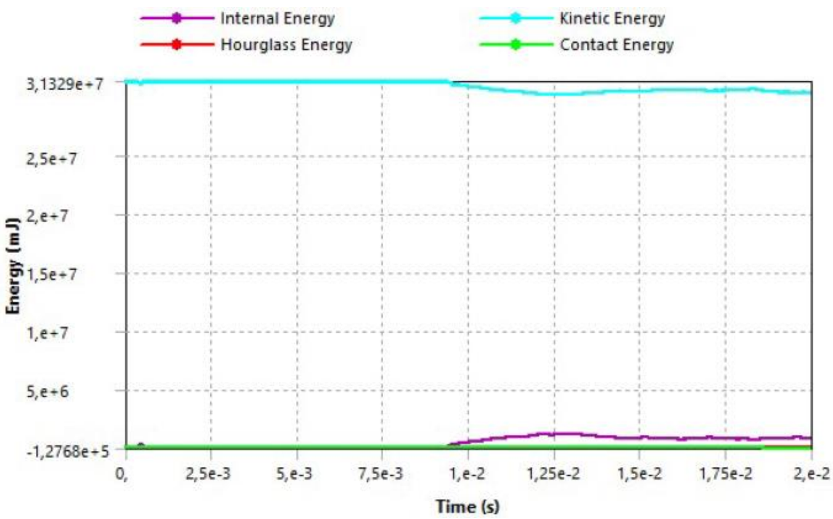

Figure 7. Energy transformation at a speed of 40 km/h

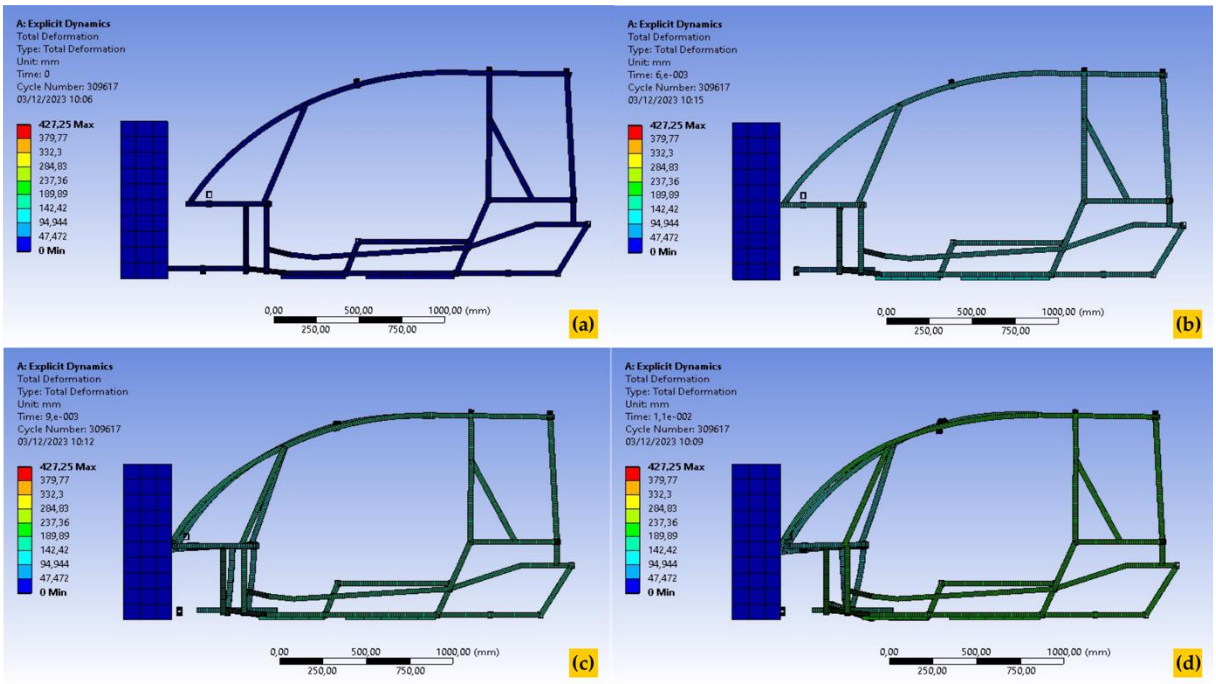

Figure 8. The car's chassis deformation: (a) 0 s; (b) 0.006 s; (c) 0.009 s; (d) 0.011 s.

Figure 8a shows that deformation does not happen at zero seconds. Figure 8b illustrates the deformation that is observed as the time increases at 0.006 s. The chassis's front zone has a maximum deformation value of 106.82 mm. As seen in Figure 8c, the highest value of deformation then rises to 168.58 mm at 0.009 s. The car's top and lower chassis are shown to be detached from their mounts at 0.011 s, as seen in Figure 8d, and the greatest deformation reaches its highest point at 203.45 mm. Table 6 provides a summary of the deformation values.

Furthermore, in Figure 8 it can be seen that by increasing the speed from 40 km/hour to 64 km/hour, the deformation value will increase. The maximum deformation that occurs at this speed is 203.45 mm. Even so, deformation only occurred in the front bumper frame and upper frame. The passenger zone is not significantly affected by this (Figure 9). The material distributes some of the energy absorbed in the front zone to the car's chassis, without distorting the proportions of the passenger zone. The energy transition is depicted in Figure 10, which also provides the energy balance graph at 64 km/h. At a speed of 40 km/h, the energy transformation pattern is nearly identical to that observed at 64 km/h. A wall causes the car's kinetic energy to drop. The automotive frame's elastic and plastic deformation causes a rise in internal energy.

Table 6. Deformation vs time at a speed of 64 km/h

Time (s)	Maximum deformation (mm)
0	0
0.006	106.82
0.009	168.58
0.011	203.45

3.2.3. *Crash Test at a Speed of 80 km/h*

In Test 3, the vehicle was driven at 80 km/h with an 8×10^{-3} second stop time. Figure 11 displays the contours of the collision impact results on the car structure before and after examination at different time steps. Since the car frame has not yet struck the barrier, no deformation is visible at the zero seconds depicted in Figure 11a. The contour in Figure 11b exhibits some distortion at 0.001 s. The front of the vehicle showed the most distortion. The deformation increases to 111.98 mm with a 0.005 s time increase (Figure 11c). The highest deformation remains in the same place with increasing time. The maximal deformation reaches its maximum value of 186.61 mm at the final time step of 0.008 s (Figure 11d). Table 7 tabulates these deformation values.

The car frame exhibits local deformation at 80 km/h, but it does not transfer to the passenger zone (Figure 12). The front zone close to the bumper frame has 186.61 mm of distortion. Energy balance graph Figure 13 shows the energy transformation. The car's kinetic energy decreases

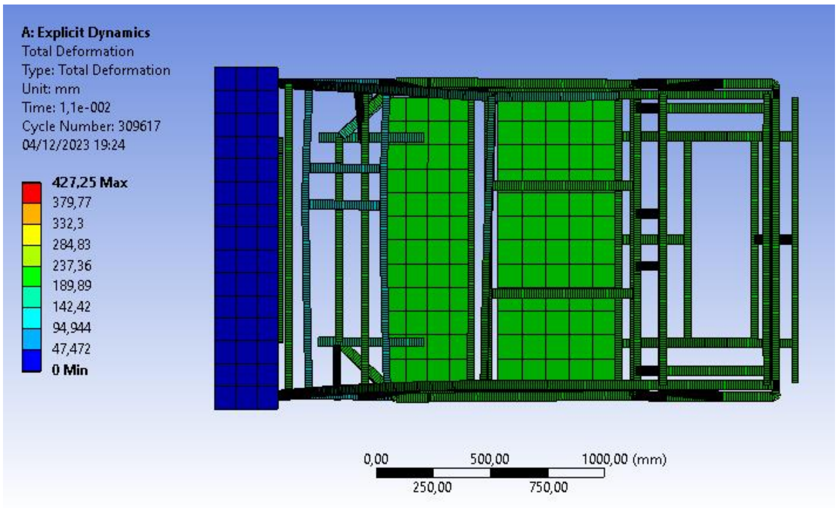

Figure 9. Deformation of the car chassis with time 0.011 s (top view)

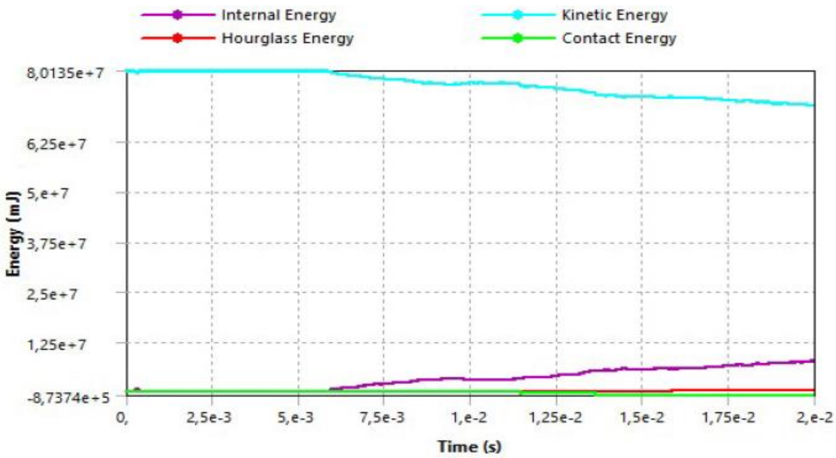

Figure 10. Energy transformation at a speed of 64 km/h

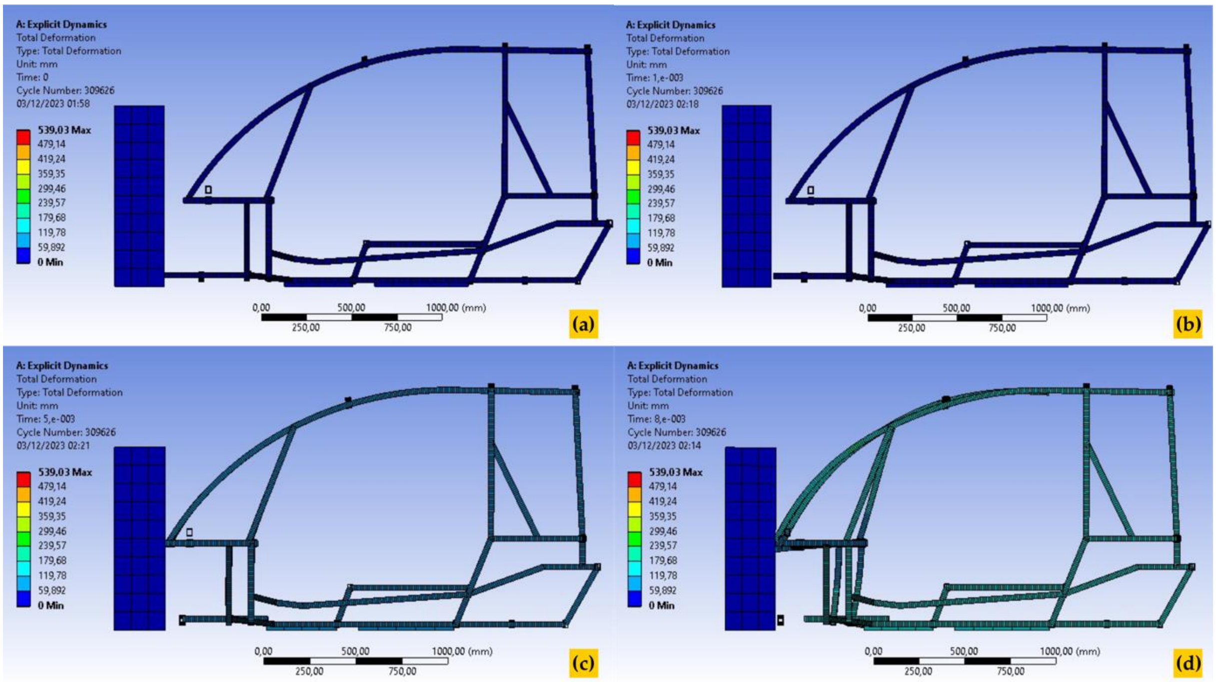

Figure 11. The car's chassis deformation: (a) 0 s; (b) 0.001 s; (c) 0.005 s; (d) 0.008 s.

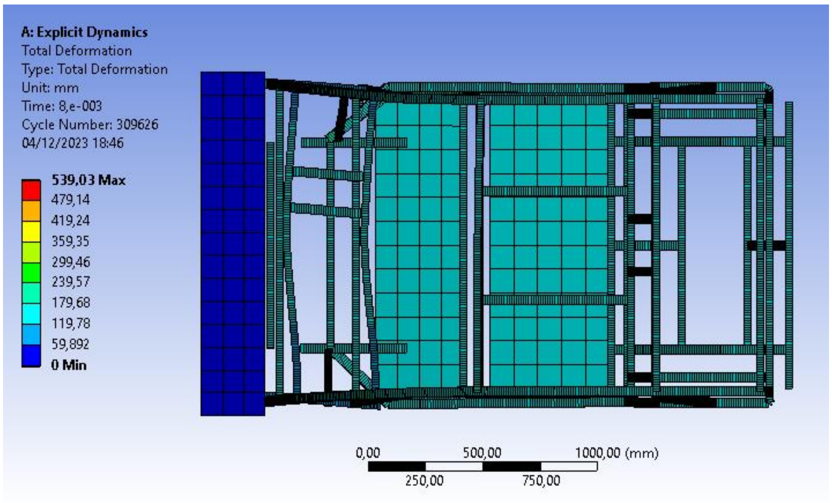

Figure 12. Deformation of the car chassis with time 0.008 s (top view)

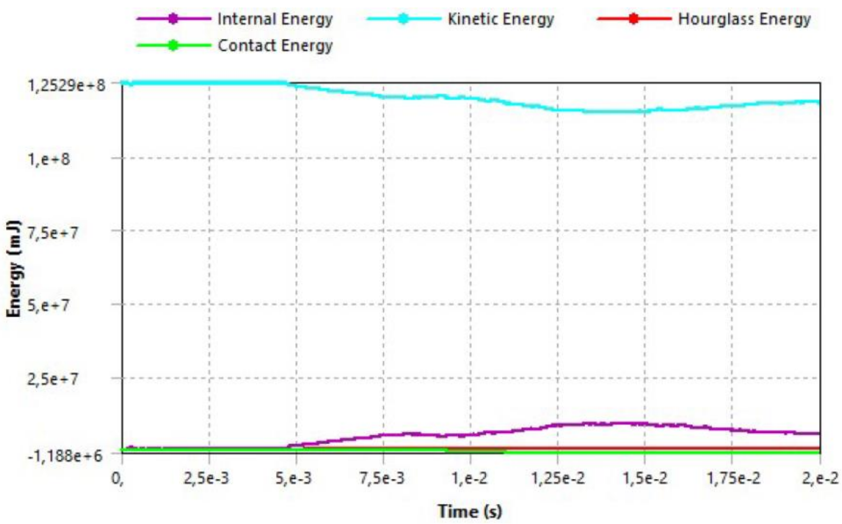

Figure 13. Energy transformation at a speed of 80 km/h

Table 7. Deformation vs time at a speed of 80 km/h

Time (s)	Maximum deformation (mm)
0	0
0.001	22.22
0.005	111.98
0.008	186.61

after hitting a wall. The automotive frame's elastic and plastic deformation causes a rise in internal energy. The system's overall energy is preserved since it is isolated. The fact that the hourglass energy is likewise within allowable bounds shows that the numerical model is valid.

3.2.4. *Crash Test at a Speed of 100 km/h*

In Test 4, the vehicle was driven at 100 km/h and stopped in 7 × 10^{-3} seconds. Figure 14 shows contours representing the impact results on the car structure before and after investigation at different time stages. There is no discernible distortion in Figure 14a. The car frame deforms at 0.0035 s, as shown in Figure 14b, with the front bumper frame of the vehicle experiencing the most deformation, measuring 97.196 mm, just like in the preceding instance. As seen in Figure 14c, the maximum deformation occurs at 0.0056 s and reaches 161.22 mm. At 0.0070 s a maximum deformation of 203.51 mm was recorded at the top pillar of the car (Figure 14d). Maximum deformation values are listed in Table 8.

Table 8. Deformation vs time at a speed of 100 km/h

Time (s)	Maximum deformation (mm)
0	0
0.0035	97.196
0.0056	161.22
0.0070	203.51

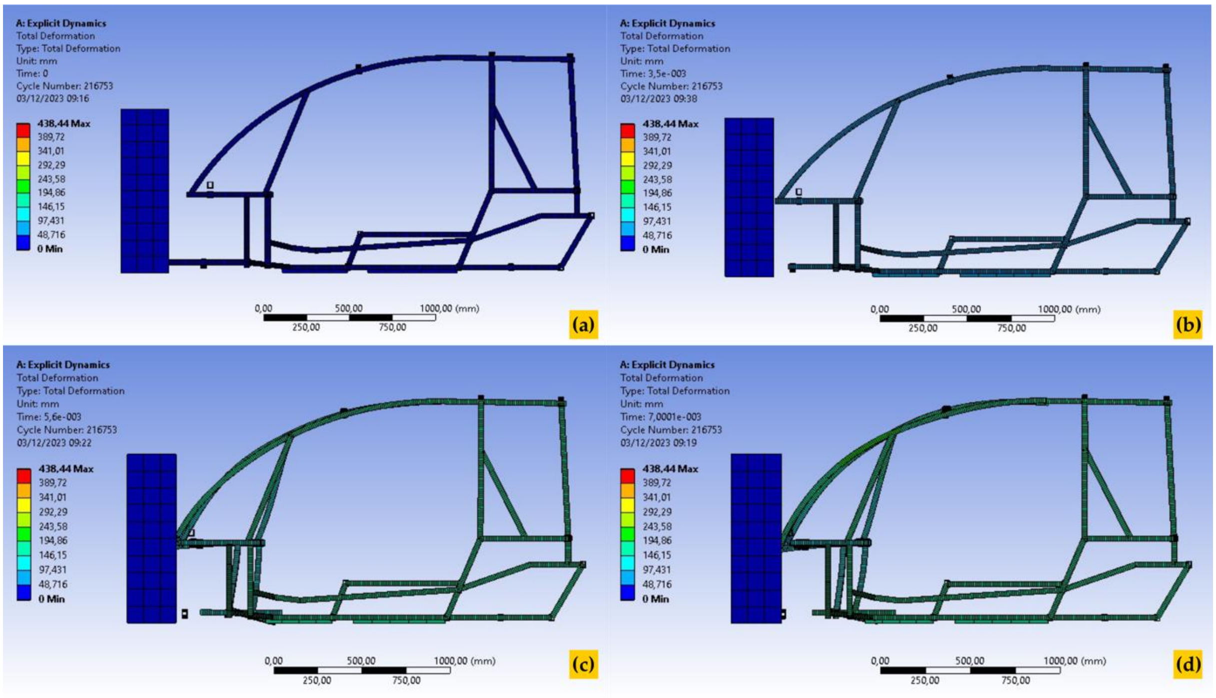

Figure 14. The car's chassis deformation: (a) 0 s; (b) 0.0035 s; (c) 0.0056 s; (d) 0.007 s

The car deforms more when traveling at 100 km/h than when traveling at 80 km/h. The car's center experienced a shift in the greatest deformation measured, which was 203.51 mm, from the front zone. The roof frame of the vehicle exhibits a small distortion in the passenger zone (**Figure 15**). The extended contact time with the wall causes a variation in the deformation pattern as compared to a speed of 80 km/h. Meanwhile, **Figure 16** shows the energy transformation at a speed of 100 km/hour. As shown in the **Figure 16**, the car's frame loses kinetic energy as it strikes the wall. In the meantime, the automobile frame's elastic and plastic deformation causes a rise in internal energy. The system's overall energy is preserved since it is isolated. The fact that the hourglass energy is likewise within allowable bounds shows that the numerical model is valid.

4. Conclusion

This study aims to design a city vehicle frame with a capacity of two passengers and test the durability of the frame in a crash test. Based on the results of the study, the dimensions of the vehicle frame are 2.46 meters long, 1.33 meters high, and 1.39 meters wide. These dimensions determine the overall size and proportion of the vehicle frame

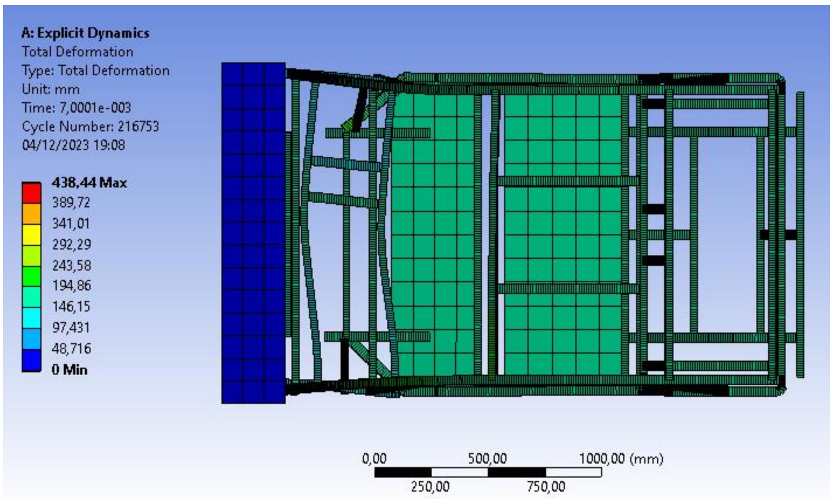

Figure 15. Deformation of the car chassis with time 0.007 s (top view)

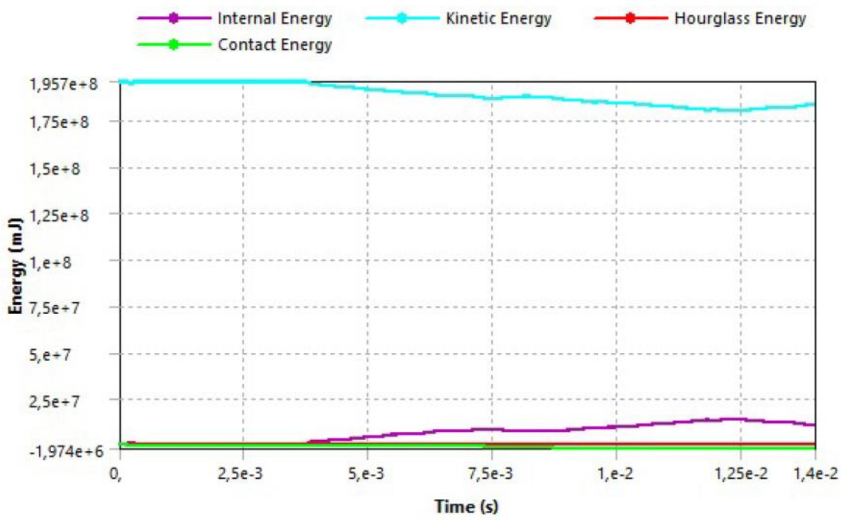

Figure 16. Energy transformation at a speed of 100 km/h

structure, where the length of the frame affects the distance between the front and rear of the vehicle, while the height and width affect the overall size of the vehicle. ASTM A36 steel material was selected in the numerical analysis of the vehicle frame because of its good strength and durability and is commonly used in the construction and automotive industries. Crash tests conducted at speeds of 40 km/h, 64 km/h, 80 km/h, and 100 km/h showed that increasing speed causes increased deformation of the frame, with a maximum deformation reaching 203.51 mm at a speed of 100 km/h. However, this deformation only occurs in the front zone of the frame and does not have a significant impact on the passenger zone. The material can absorb some of the deformation, with most of the energy transferred to the vehicle structure, keeping the dimensions of the passenger zone relatively safe. Future research will focus on the interaction of lightweight materials with frame structures in crash situations, with an emphasis on a variety of innovative materials such as carbon composites and nanotechnology for stronger, lighter, and more environmentally friendly vehicle frame designs.

Acknowledgement

The Authors would like to thank Lembaga Penelitian dan Pengabdian Masyarakat Universitas Negeri Padang for Funding this work with contract number: 2122/UN35.15/LT/2023.

Author's Declaration

Authors' contributions and responsibilities

The authors made substantial contributions to the conception and design of the study. The authors took responsibility for data analysis, interpretation and discussion of results. The authors read and approved the final manuscript.

Funding

This research was funded by Lembaga Penelitian dan Pengabdian Masyarakat, Universitas Negeri Padang through a research group grant scheme with contract number: 2122/UN35.15/LT/2023.

Availability of data and materials

All data are available from the authors.

Competing interests

The authors declare no competing interest.

Additional information

No additional information from the authors.

References

[1] A. D. Furlan *et al.*, "Advanced vehicle technologies and road safety: A scoping review of the evidence," *Accident Analysis & Prevention*, vol. 147, p. 105741, Nov. 2020, doi: 10.1016/j.aap.2020.105741.

[2] L. Wang, H. Zhong, W. Ma, M. Abdel-Aty, and J. Park, "How many crashes can connected vehicle and automated vehicle technologies prevent: A meta-analysis," *Accident Analysis & Prevention*, vol. 136, p. 105299, Mar. 2020, doi: 10.1016/j.aap.2019.105299.

[3] J. Moody, N. Bailey, and J. Zhao, "Public perceptions of autonomous vehicle safety:

An international comparison," *Safety Science*, vol. 121, pp. 634–650, Jan. 2020, doi: 10.1016/j.ssci.2019.07.022.

[4] M. S. Parvez, M. M. Rahman, M. Samykano, and M. Y. Ali, "Current advances in fabric-based airbag material selection, design and challenges for adoption in futuristic automobile applications," *Materials Today: Proceedings*, Sep. 2023, doi: 10.1016/j.matpr.2023.09.081.

[5] D. W. Karmiadji, M. Gozali, M. Setiyo, T. Raja, and T. A. Purnomo, "Comprehensive Analysis of Minibuses Gravity Center: A Post-Production Review for Car Body Industry," *Mechanical Engineering for Society and Industry*, vol. 1, no. 1, pp. 31–40, 2021, doi: 10.31603/mesi.5250.

[6] H. S. Hanandita, U. Ubaidillah, A. R. Prabowo, B. W. Lenggana, A. Turnip, and E. Joelianto, "Static Structural Analysis of Checking Fixture Frame of Car Interior Using Finite Element Method," *Automotive Experiences*, vol. 6, no. 3, pp. 652–668, 2023, doi: 10.31603/ae.9860.

[7] F. Endrasari, D. W. Djamari, B. A. Budiman, and F. Triawan, "Rollover Stability Analysis and Layout Optimization of a Delta E-trike," *Automotive Experiences*, vol. 5, no. 2, pp. 137–149, Mar. 2022, doi: 10.31603/ae.6136.

[8] I. Ansori *et al.*, "Enhancing Brake System Evaluation in Periodic Testing of Goods Transport Vehicles through FTA-FMEA Risk Analysis," *Automotive Experiences*, vol. 6, no. 2, pp. 320–335, Aug. 2023, doi: 10.31603/ae.8394.

[9] R. Majuma, M. H. Bin Peeie, K. Ondong, and O. A. Hassan, "Investigation of Brake Pad Wear Effect due to Temperature Generation Influenced by Brake Stepping Count on Different Road Terrains," *Automotive Experiences*, vol. 6, no. 2, pp. 234–244, May 2023, doi: 10.31603/ae.8869.

[10] A. R. Zubir, K. Hudha, Z. A. Kadir, and N. H. Amer, "Enhanced Modeling of Crumple Zone in Vehicle Crash Simulation Using Modified Kamal Model Optimized with Gravitational Search Algorithm," *Automotive Experiences*, vol. 6, no. 2, pp. 372–383, Aug. 2023, doi: 10.31603/ae.9289.

[11] J. Répás and L. Berek, "Security and Safety Systems on Modern Vehicles," in *Vehicle and Automotive Engineering 4. VAE 2022. Lecture Notes in Mechanical Engineering*, 2023, pp. 84–100.

[12] M. Mackay, "Current Vehicle Safety Technologies and Future Directions," in *Transport and Safety*, 2021, pp. 189–203.

[13] G. Refiadi, I. S. Aisyah, and J. P. Siregar, "Trends in lightweight automotive materials for improving fuel efficiency and reducing carbon emissions," *Automotive Experiences*, vol. 2, no. 3, pp. 78–90, 2019, doi: 10.31603/ae.v2i3.2984.

[14] A. D. Shieddieque, I. Rahayu, S. Hidayat, and J. A. Laksmono, "Recent Development in LiFePO4 Surface Modifications with Carbon Coating from Originated Metal-Organic Frameworks (MOFs) to Improve the Conductivity of Cathode for Lithium-Ion Batteries: A Review and Bibliometrics Analysis," *Automotive Experiences*, vol. 6, no. 3, pp. 438–451, 2023, doi: 10.31603/ae.9524.

[15] A. D. Shieddieque, Sukarman, Mardiyati, B. Widyanto, and Y. Aminanda, "Multi-objective Optimization of Sansevieria Trifasciata FibreReinforced Vinyl Ester (STF/VE) Bio-composites for the Sustainable Automotive Industry," *Automotive Experiences*, vol. 5, no. 3, pp. 288–303, 2022, doi: 10.31603/ae.7002.

[16] S. N. S. Z. Abidin, W. H. Azmi, N. N. M. Zawawi, and A. I. Ramadhan, "Comprehensive Review of Nanoparticles Dispersion Technology for Automotive Surfaces," *Automotive Experiences*, vol. 5, no. 3, pp. 304–327, Jun. 2022, doi: 10.31603/ae.6882.

[17] R. P. Putra, D. Yuvenda, M. Setiyo, A. Andrizal, and M. Martias, "Body City Car Design of Two Passengers Capacity: A Numerical Simulation Study," *Automotive Experiences*, vol. 5, no. 2, pp. 163–172, 2022, doi: 10.31603/ae.6304.

[18] M. Aoto, Y. Wada, and Y. Numata, "Development of an FPGA Controlled 'Mini-Car' Toward Autonomous Driving," in *2018 International Conference on Field-Programmable Technology (FPT)*, Dec. 2018, pp. 400–402, doi: 10.1109/FPT.2018.00084.

[19] V. Saplinova, I. Novikov, and S. Glagolev,

"Design and specifications of racing car chassis as passive safety feature," *Transportation Research Procedia*, vol. 50, pp. 591–607, 2020, doi: 10.1016/j.trpro.2020.10.071.

[20] T. A. Babu, D. V. Praveen, and Dr.M Venkateswarao, "Crash analysis of car chassis frame using finite element method," *International Journal of Engineering Research & Technology*, vol. 1, no. 8, pp. 1–8, 2012.

[21] W. A. Wirawan, B. Junipitoyo, S. H. S. Putro, A. H. Suudy, R. Ridwan, and M. A. Choiron, "Collapse Behavior and Energy Absorption Characteristics of Design Multi-Cell Thin Wall Structure 3D-Printed Under Quasi Statistic Loads," *Automotive Experiences*, vol. 7, no. 1, pp. 149–160, 2024, doi: 10.31603/ae.10892.

[22] K. Podkowski, A. Małczuk, A. Stasiak, and M. Pawlak, "Testing of the torsional stiffness of the passenger car frame and its validation by means of finite element analysis," *The Archives of Automotive Engineering – Archiwum Motoryzacji*, vol. 85, no. 3, pp. 83–101, Sep. 2019, doi: 10.14669/AM.VOL85.ART6.

[23] Akshay Dehankar, Yogesh Ingole, Abhijit Turkane, and Aniket Nandurkar, "A Review on modern vehicle Virtual Crash Test to Understand the Effect of Impact on Passengers," *International Journal of Scientific Research in Science and Technology*, vol. 9, no. 2, pp. 289–294, Apr. 2022, doi: 10.32628/IJSRST229176.

[24] M. A. Basith, N. C. Reddy, S. Uppalapati, and S. P. Jani, "Crash analysis of a passenger car bumper assembly to improve design for impact test," *Materials Today: Proceedings*, vol. 45, pp. 1684–1690, 2021, doi: 10.1016/j.matpr.2020.08.561.

[25] D. S. Dima and D. Covaciu, "Vehicles Frontal Impact Analysis Using Computer Simulation and Crash Test," *International Journal of Automotive Technology*, vol. 20, no. 4, pp. 655–661, Aug. 2019, doi: 10.1007/s12239-019-0062-3.

[26] T. P. Hutchinson, "Full Frontal Car Crash Tests: Empirical Evidence about Shape of Deceleration Pulses," *International Journal of Automotive Technology*, vol. 22, no. 2, pp. 383–389, Apr. 2021, doi: 10.1007/s12239-021-0036-0.

[27] P. Kubiak, K. Siczek, A. Dąbrowski, and A. Szosland, "New high precision method for determining vehicle crash velocity based on measurements of body deformation," *International Journal of Crashworthiness*, vol. 21, no. 6, pp. 532–541, Nov. 2016, doi: 10.1080/13588265.2016.1194566.

[28] B. Barabino, M. Bonera, G. Maternini, A. Olivo, and F. Porcu, "Bus crash risk evaluation: An adjusted framework and its application in a real network," *Accident Analysis & Prevention*, vol. 159, p. 106258, Sep. 2021, doi: 10.1016/j.aap.2021.106258.

[29] R. Mirzaamiri, M. Esfahanian, and S. Ziaei-Rad, "Crash Test Simulation and Structure Improvement of IKCO 2624 Truck According to ECE-R29 Regulation," *International Journal of Automotive Engineering*, vol. 2, no. 3, pp. 180–192, 2012.

[30] R. Thomson, R. Fredriksson, K. Mroz, D. Kruse, and F. Törnvall, "Frontal Crash Incompatibility of Heavy Goods Vehicle in Crash Test With Passenger Car," 2023.

[31] T. M. Bosire, "Vehicle Structure Designs and Materials on School Bus Body Crashworthiness: A Case of Vehicle Body Building Industry in Nairobi County, Kenya," University of Eldoret, Kenya, 2021.

[32] G. Genta and L. Morello, *The Automotive Chassis*. Dordrecht: Springer Netherlands, 2009.

[33] N. Asadinia, A. Khalkhali, and M. J. Saranjam, "Sensitivity analysis and optimization for occupant safety in automotive frontal crash test," *Latin American Journal of Solids and Structures*, vol. 15, no. 7, Jul. 2018, doi: 10.1590/1679-78254666.

[34] D. S. Dima and D. Covaciu, "Solutions for acceleration measurement in vehicle crash tests," *IOP Conference Series: Materials Science and Engineering*, vol. 252, p. 012007, Oct. 2017, doi: 10.1088/1757-899X/252/1/012007.

[35] Chan En Lim, Kok Hing Chong, Charlie Chin Voon Sia, Yeu Yee Lee, and Man Djun Lee, "Numerical Study for Crashworthiness of FSAE Vehicle Chassis via Biomimetic Approach," *Journal of Advanced Research in*

Applied Sciences and Engineering Technology, vol. 33, no. 2, pp. 328–339, Nov. 2023, doi: 10.37934/araset.33.2.328339.

[36] R. P. Putra, Waskito, D. Yuvenda, and J. Adri, "Stress analysis of the frame of a corn harvesting tractor," *EUREKA: Physics and Engineering*, no. 6, pp. 47–58, Nov. 2023, doi: 10.21303/2461-4262.2023.002862.

[37] U. Idrees *et al.*, "Finite element analysis of car frame frontal crash using lightweight materials," *Journal of Engineering Research*, vol. 11, no. 1, p. 100007, Mar. 2023, doi: 10.1016/j.jer.2023.100007.